EUROPEAN LABORATORY FOR PARTICLE PHYSICS

CERN – AB DIVISION

AB-Note-2003-014 OP

Energy Calibration of the SPS at 450 GeV/c with Proton and Lead Ion Beams

G. Arduini, C. Arimatea, T. Bohl, P. Collier, K. Cornelis, J. Wenninger

Abstract

The momentum of the SPS proton beam at 450 GeV/c, corresponding to the extraction energy for the LHC, was determined by a measurement of the revolution frequencies of proton and lead ion beams. To maximize the sensitivity of the measurement, non-fully stripped Pb^{53+} was injected into the same magnetic cycle than the proton beams. The beam momentum was determined from the RF frequency for which the beams are centered in the machine sextupoles. The measured beam momentum is 449.16 ± 0.14 GeV/c for a nominal momentum of 450 GeV/c. The accuracy is limited by systematic differences observed for measurements in the horizontal and vertical planes.

Geneva, Switzerland

February 3, 2003

1 Introduction

Since the shutdown of LEP at the end of 2000, the SPS machine is modified and adapted to its role as injector for the LHC collider. As LHC injector, the SPS must deliver very bright beams with high efficiency and without emittance degradation to both LHC rings. The machine model is re-measured in details and as part of this effort, the beam momentum at the extraction energy of 450 GeV/c was calibrated in order to obtain the best possible initial energy setting when the LHC will be commissioned. Advantage was taken of the last lead ion run in the SPS before the startup of the LHC in 2007. To enhance the sensitivity of the measurement, the calibration was performed with Pb^{53+} instead of the fully stripped Pb^{82+} that is used for fixed target physics.

This note begins with a brief description of the momentum calibration method. The measurement conditions are explained and finally the results for the SPS beam momentum are given and discussed.

2 Calibration Principle

The goal of the energy calibration is the determination of the beam momentum on the central orbit, where the beam is centered on average in the machine quadrupoles. On this orbit the momentum is entirely determined by the dipole field and the measurement of the beam momentum under such conditions provides a calibration of the integrated field of the main dipoles.

The calibration principle that is used here relies on the measurement of the revolution frequency of two ion species with different charge over mass ratio, and therefore different speed and revolution frequency, that are injected into the same magnetic machine. Such a technique was used very successfully at LEP with protons and positrons [1]. The momentum is determined from the central RF frequency setting where the beam is centered on average in the machine quadrupoles, even tough in practice the central RF frequency is actually determined by centering the beams in the machine sextupoles. For that RF frequency value, the transverse tune no longer depends on the setting of the chromaticity. For a sufficiently large number of sextupoles and a correct alignment of the sextupoles with respect to the quadrupoles, the beam should be centered in the sextupoles and quadrupoles at the same time. Systematic alignment effects can be probed by performing the measurement for the horizontal plane and for the vertical plane independently. More details will be given in the next section.

The speed of the particles βc, where c is the speed of light, can be related to the revolution frequency f_{rev} and the corresponding RF frequency f_{RF} through

$$\beta c = C f_{rev} = \frac{C f_{RF}}{h} \tag{1}$$

where h is the harmonic number of the RF system, $h = 4620$ for the SPS. C is the machine circumference. It is evident from this equation that to determine the speed β and therefore the particle momentum, both the machine circumference and the revolution frequency must be known. To determine momentum and machine circumference at the same time, the revolution frequency is measured for two particles with different masses (or charge over mass ratio) that are injected into exactly the same magnetic machine and on the same orbits. In our case the measurements are performed for a proton and an lead ion beam.

The speed $\beta_p c$ of the proton beam is related to its momentum P, the main parameter of interest, and its rest mass m_p by

$$\beta_p^2 = \frac{P^2}{P^2 + (m_p c)^2} \ . \tag{2}$$

An ion beam of charge Z, injected into the same magnetic machine and on the same orbit than the proton beam has a momentum $P_i = ZP$. We define the proton equivalent momentum of the ion as $P = P_i/Z$. The speed $\beta_i c$ of the ions is given by

$$\beta_i^2 = \frac{P^2}{P^2 + (m_i c/Z)^2} \tag{3}$$

with m_i the ion rest mass. The two equations for β_p and β_i can be solved for the proton beam momentum P, yielding

$$P = m_p c \sqrt{\frac{\kappa^2\mu^2 - 1}{1 - \kappa^2}} \tag{4}$$

with

$$\kappa = \beta_i/\beta_p = f^i_{RF}/f^p_{RF} \tag{5}$$

and

$$\mu = \frac{m_i}{Z m_p} \ . \tag{6}$$

$1/\mu$ is the number of charges per nucleon of the ion. For Pb^{53+} ions $\mu \simeq 4$, while for fully stripped lead ions Pb^{82+}, $\mu \simeq 2.5$.

Equation 4 can be approximated by

$$P \cong m_p c \sqrt{\frac{f^p_{RF}}{2\Delta f}(\mu^2 - 1)} \tag{7}$$

where the RF frequency difference $\Delta f = f^p_{RF} - f^i_{RF}$ between the beams has been introduced. The measurement error σ_P on P is dominated by the term

$$\frac{\sigma_P}{P} \simeq \frac{\sqrt{\sigma^2_{f^p_{RF}} + \sigma^2_{f^i_{RF}}}}{2\ \Delta f} \tag{8}$$

with $\sigma_{f^p_{RF}}$ and $\sigma_{f^i_{RF}}$ the measurement errors on the central RF frequencies of the proton and ion beams. All other contributions to σ_P are very small, in particular the uncertainties due to the particle masses. Equation 8 clearly indicates the need to maximize the frequency difference to obtain the best possible accuracy for a given error on the central frequency determination. For highly relativistic beams where β_p and β_i and very close to 1,

$$\beta_p^2 = 1 - (\frac{m_p c}{P})^2 + ... \quad \text{and} \quad \beta_i^2 = 1 - (\frac{m_i c}{ZP})^2 + ... \ , \tag{9}$$

the frequency difference is given approximately by

$$\Delta f = \frac{hc}{C}(\beta_p - \beta_i) \simeq \frac{h m_p^2 c^3}{2CP^2}(\mu^2 - 1) \tag{10}$$

and scales quadratically with μ. Note also the dependence on $1/P^2$ which makes the measurement very difficult at high energy when both beam are highly relativistic.

3 Machine Preparation and Measurements

The momentum calibration was performed for the SPS LHC beam cycle (SC no. 540) with a total length of 21.6 seconds. The beams are injected at 26 GeV/c and accelerated to 450 GeV/c in approximately 8 seconds. The settings of all magnet were kept rigorously identical for both proton and lead beams, except for the chromaticity which had to be varied to determine the central frequency.

Under normal running conditions for fixed target experiments in the SPS, Pb^{53+} is accelerated in the PS to a proton equivalent momentum P_{Pb}/Z of 19.8 GeV/c, corresponding to a lead ion momentum P_{Pb} of 53 $\times$ 19.8 GeV/c $\simeq$ 1.05 TeV/c. The extracted lead beam is fully tripped to Pb^{82+} in the transfer line between PS and SPS. In the SPS the fully stripped Lead beam has a momentum P_{Pb}/Z of 12.9 GeV/c since its total momentum of 82 $\times$ 12.9 GeV/c = 1.05 TeV/c is unchanged. To maximize the frequency difference Δf for the calibration, the lead beam was not stripped in the transfer line and injected as Pb^{53+} into the SPS. Furthermore the beam was accelerated in the PS to the LHC beam injection momentum P_{Pb}/Z of 26 GeV/c, since no stripping is performed in the transfer line. The lifetime of Pb^{53+} in the SPS was 5.3 seconds at P_{Pb}/Z of 26 GeV/c, limited by the vacuum conditions. To accelerate the Pb^{53+} to P_{Pb}/Z of 450 GeV/c, the RF capture and acceleration had to be re-tuned, an operation that took several hours.

In Nature the most common lead isotope is Pb_{208} with an abundance of $\sim$ 52%, while isotopes Pb_{207} and Pb_{206} have a natural abundance of slightly over 20% each. The lead ion source is composed of isotopically pure ($> 96\%$) Pb_{208} [10].

At 450 GeV/c the closed orbit r.m.s in the SPS was 2.0 and 1.5 mm for the horizontal and vertical planes, see also Figure 4. The transverse tunes were set to $Q_h = 26.18$ and $Q_v = 26.14$. The current setting of the main dipoles magnets was 5756.02 A. The magnetic field in the reference dipole was measured with an NMR probe. The field was stable at 2.0251 ± 0.0002 T during the 2 days of measurements.

The proton beam intensities corresponded to $\sim 10^{11}$ protons per bunch. The total Pb^{53+} ion beam intensity was only $\sim 3 - 5\ 10^9$ charges distributed over 2 batches.

3.1 Central Frequency Measurements

The central RF frequency is obtained in the following way. For a number of different chromaticity settings (positive and negative), the tune is measured as a function of the radial position (RF frequency) within a small window around the central RF frequency. For the analysis the range of radial excursions is limited to avoid entering a regime of non-linear chromaticity. For each chromaticity and RF frequency setting, the tune is recorded 150 ms before the beam is dumped at the end of the cycle.

For the LHC proton beam the RF frequency program used for the acceleration is based on a programmed frequency synthesizer. The cycle to cycle fluctuation of the RF frequency is smaller than 1 Hz. For the lead beams however, a radial loop is used to control the radial steering of the beam during the cycle. Due to the intensity dependance of the RF pickup, the radial steering (and therefore the RF frequency) fluctuates from one cycle to the next by up to 20 Hz. With lead beams it is therefore important to record simultaneously the tune and the RF frequency during the same cycle.

For each chromaticity setting, the tune dependence on the RF frequency should be linear.

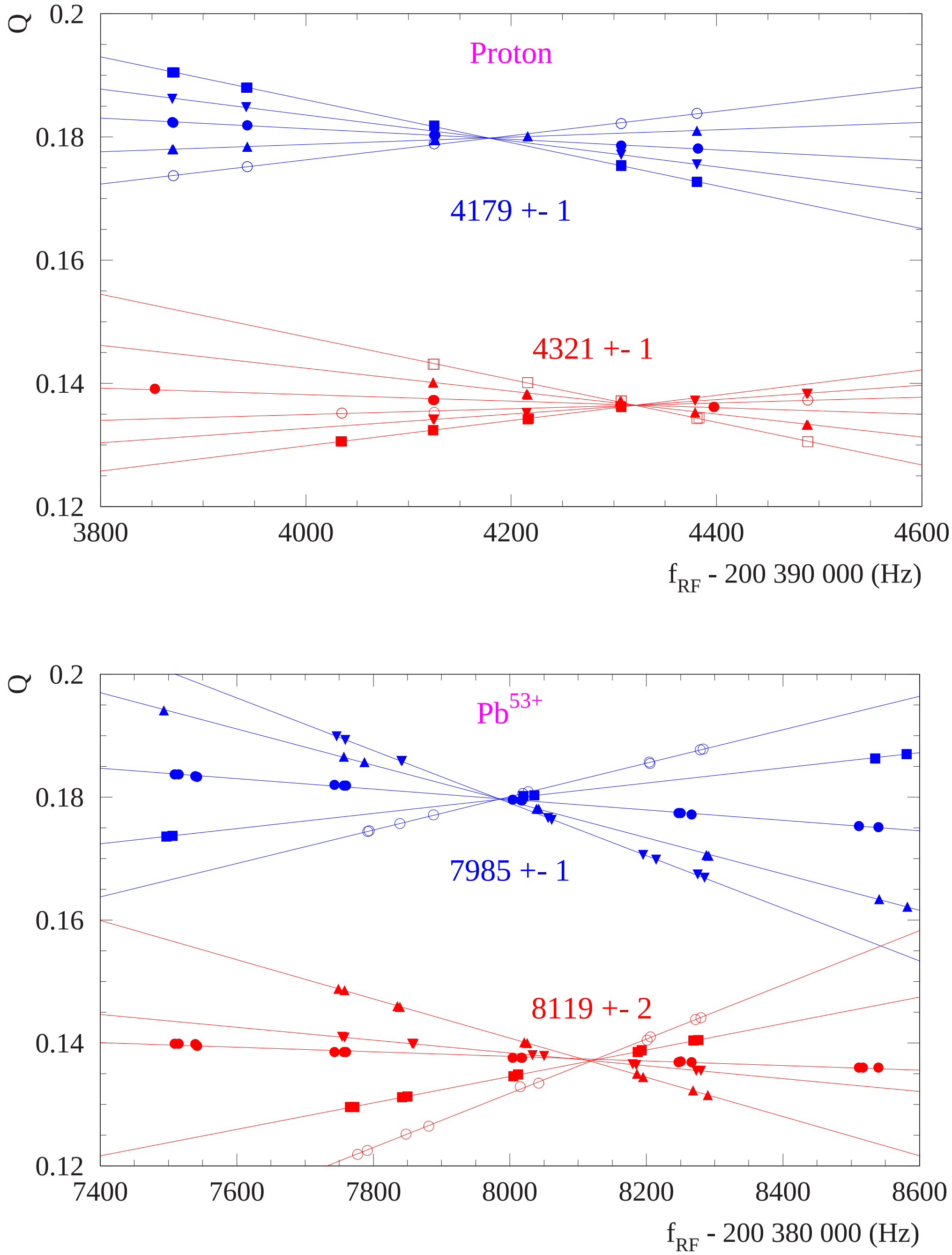

Figure 1: Tune dependence on RF frequency for different settings of the machine chromaticity for proton (top) and Pb^{53+} beams (bottom) at a proton equivalent momentum of 450 GeV/c. The RF frequency (and its error) that corresponds to the crossing of the lines is indicated for each measurement set (horizontal, $Q \simeq 0.18$ and vertical, $Q \simeq 0.14$).

Frequency	Plane	Raw value (Hz)	Tide shift (Hz)	Tide corrected value (Hz)
f_{RF}^{p}	Horizontal	$200'394'178.6 \pm 1.0$	-2.8	$200'394'181.4 \pm 1.0$
	Vertical	$200'394'321.1 \pm 1.0$	-0.1	$200'394'321.2 \pm 1.0$
	Vert. - Hor.	142.5 ± 1.4	$+2.7$	139.8 ± 1.4
f_{RF}^{pb}	Horizontal	$200'387'985.3 \pm 1.2$	-1.8	$200'387'987.1 \pm 1.2$
	Vertical	$200'388'119.1 \pm 2.5$	-1.7	$200'388'120.8 \pm 2.5$
	Vert. - Hor.	133.8 ± 2.8	$+0.1$	133.7 ± 2.8
$\Delta f = f_{RF}^{p} - f_{RF}^{pb}$	Horizontal	$6'193.3 \pm 1.6$	-1.0	$6'194.3 \pm 1.6$
	Vertical	$6'202.0 \pm 2.7$	$+1.6$	$6'200.4 \pm 2.7$
	Vert. - Hor.	8.7 ± 3.1	$+2.6$	6.1 ± 3.1

Table 1: Summary table of central frequency results. The measured raw values are indicated in the third column, while the values corrected for the tidal shifts are given in the last rightmost column.

The central RF frequency corresponds to the crossing point of all the lines obtained for all chromaticity settings, as can be seen in Figure 1. The measurement series is repeated twice, once for horizontal chromaticity changes where the horizontal tune is recorded, once for vertical changes where the vertical tune is recorded. A zoom on the crossing point is shown for the horizontal proton data in Figure 2.

The chromaticity is corrected in the SPS using 108 lattice sextupoles, 54 LSD type (vertical focusing) and 54 LSF type (horizontal focusing) magnets. The LSD magnets are grouped in 2 families, LSDA (18 magnets) and LSDB (36 magnets). The LSF are grouped in 3 families, LSFA (24 magnets), LSFB (18 magnets) and LSFC (12 magnets). For the super-cycles and optics considered for this note, the strengths of LSFA and LSFC families are identical. The total number of SPS lattice quadrupoles is 216, i.e. there is only one sextupole for 2 quadrupoles. Since horizontal chromaticity changes are mainly performed using the LSF sextupoles, while the vertical chromaticity is mainly varied using the LSD family, the central frequencies obtained from the two planes are determined by the alignment of those two families. Differences in central frequency between horizontal and vertical planes are an indication for the size of the alignment errors between families.

The tune data sets are shown in Figure 1 for the two beams. The data quality is excellent and the crossing points of the chromaticity curves are determined with an accuracy of $1-2$ Hz. The raw results are given in Table 1. The frequency difference between protons and lead ions is approximately 6.2 kHz. Two systematic effects are apparent in the data. First, the central frequencies determined from the two planes differ by approximately 140 Hz. Secondly the frequency difference between proton and lead beams is not entirely consistent within the errors between the two planes, the difference being approximately 3 times larger than the estimated error.

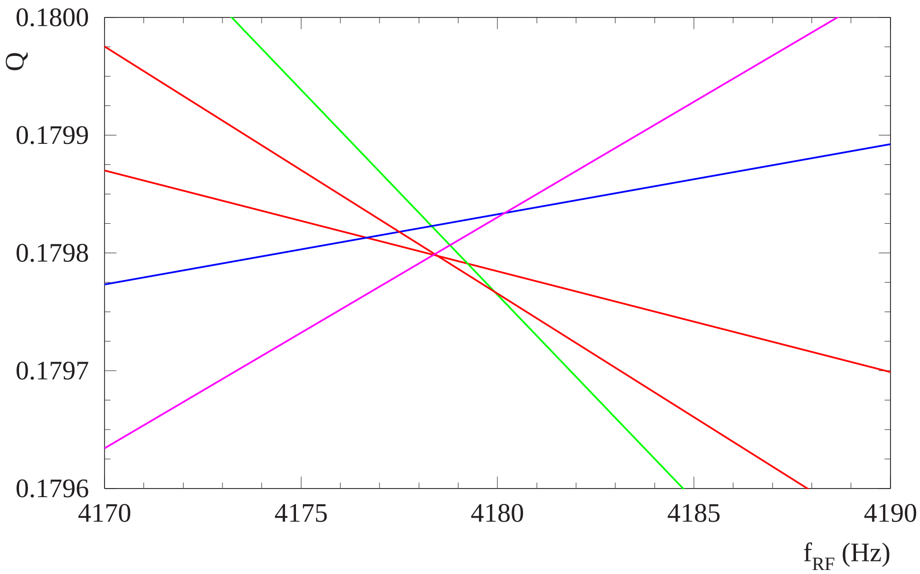

Figure 2: Zoom on the crossing point of the chromaticity lines for the horizontal proton data.

4 SPS Beam Momentum

4.1 Earth Tides

Large accelerators and storage rings are subject to radial deformations due to Earth tides, an effect that has been clearly demonstrated for LEP, where the tidal distortions contributed significantly to the LEP beam energy fluctuations [2]. For LEP the tidal corrections were modelled using a CTE (Cartwright-Taylor-Edden) model which includes the 505 main tide harmonics [3]. A program based on such a tide model, where some parameters are adjusted with actual gravity measurements, is available to estimate the tidal change in gravitational acceleration Δg. The change of gravitational acceleration is related to the radial distortions through

$$\frac{\Delta C}{C} = \lambda \frac{\Delta g}{g} \tag{11}$$

where the coupling factor λ was determined to be -0.15 ± 0.01 [4], in agreement with geological models. Tidal deformations therefore induce changes of the SPS central frequency of

$$\Delta f_{RF}[\mathrm{Hz}] = f_{RF} \frac{\Delta C}{C} = \frac{\lambda\, f_{RF}\, \Delta g}{g} = (3.1 \pm 0.2)\, \Delta g[\mu\mathrm{m/s}^2] \tag{12}$$

At high tides, the local change in gravity reaches $\sim \pm 1.5$ μm/s^2, leading to central frequency changes of about $\pm$ 5 Hz in the SPS. The corresponding circumference change is $\pm$ 170 μm.

The prediction for the local gravity change due to the tides is shown in Figure 3 for the 7 day period around the energy measurement that in fact coincided with a period of Full Moon. Due to the inclination of the Earth rotation axis and of the plane of the lunar orbit with respect to the plane of the Ecliptic, the highest Earth tides do not necessarily coincide with New Moon

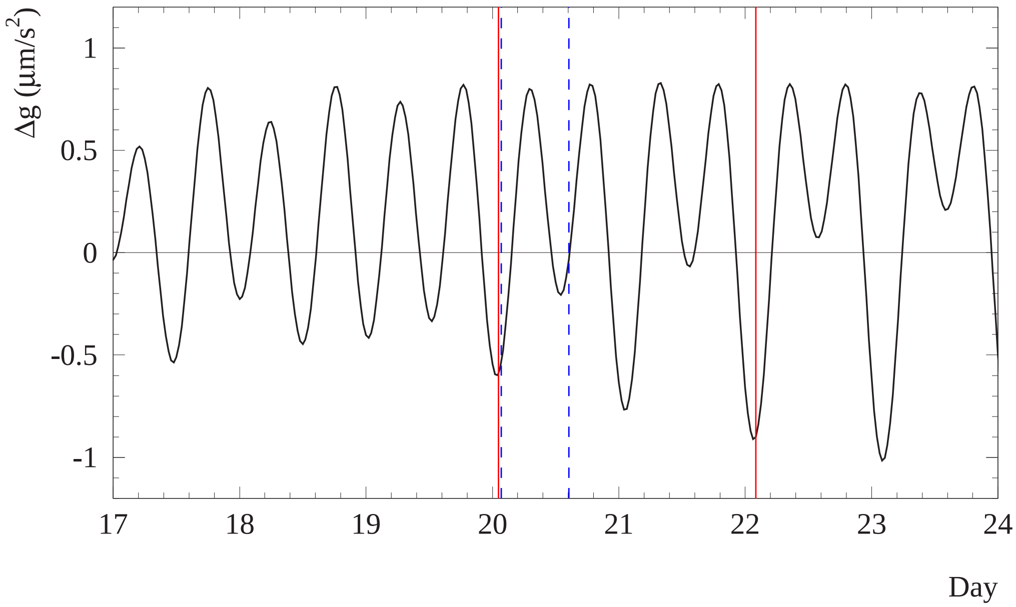

Figure 3: Evolution of the gravity change due to tidal distortions in Geneva between October 17^{th} and October 24^{th} 2002. Full moon is at 8 a.m. on October 21^{st}. Solid vertical lines correspond to the horizontal plane measurements, dotted lines to vertical plane measurements. The first two measurements correspond to lead ions, the other measurements to protons.

or Full Moon which are defined by the geometrical alignment of Moon, Earth and Sun. The tide corrections to the central frequency values are given in Table 1. After correction of the tidal effects, the agreement of the Δf values for the two planes is improved, the systematic difference being reduced from 3 to 2 standard deviations.

4.2 Beam Momentum and Machine Circumference

The measured central RF frequencies can be converted to beam energies using the proton and lead ion masses given in Table 2. For Pb^{53+} the atomic mass data of lead isotope 208 must be corrected for the missing 29 electrons. The two fundamental parameters, namely the proton momentum P and the central orbit length are obtained from equations 1 and 4. The results are given in Table 3 for both horizontal and vertical planes. Due to the differences observed between the planes, the numbers do not agree within their errors, in particular for the machine circumference. For the beam momentum, the numbers from the two planes agree within 2 standard deviations, which is acceptable. A conservative approach is adopted and the systematic difference is taken into account by averaging the results for the two planes. Half the difference between the measurements for the two planes is used as systematic error and is propagated to all derived quantities.

The uncertainty of $\sigma_C \simeq 2.4$ mm on the length of the central orbit due to the systematic effects between the two planes contributes an additional uncertainty to the momentum of the beam. This uncertainty is given by

$$\sigma_P = P\frac{\sigma_C}{\alpha C} = 0.08\ \mathrm{GeV/c} \tag{13}$$

Parameter	Symbol	Value
Proton mass [5] (MeV/c^2)	m_p	$938.271998(38)$
Electron mass [5] (MeV/c^2)	m_e	$0.510998902(21)$
Atomic mass unit [5](MeV/c^2)	m_u	$931.494013(37)$
Pb_{208} atomic mass [6]	m_{pb}/m_u	$207.976639(3)$
Pb_{208}^{53+} atomic mass	m_{pb53+}/m_u	$207.960730(3)$
$\mu = m_{pb53+}/Zm_p$ ($Z = 53$, Eq. 6)		$3.8954423(3)$
Speed of light [5] (m/s)	c	299792458

Table 2: Fundamental parameters that are used to extract the beam momentum from the central frequency measurements. The errors on the parameters are given in parenthesis. For this measurement the atomic mass of Pb_{208} must be corrected for the 29 missing electrons.

Parameter	Value		
	Horizontal plane	Vertical plane	Difference
Proton momentum P (GeV/c)	449.265 ± 0.057	449.044 ± 0.098	0.221 ± 0.113
Central orbit length C (mm)	$6'911'568.62 \pm 0.04$	$6'911'563.78 \pm 0.04$	4.84 ± 0.05

Table 3: Proton beam momentum and central orbit length obtained from the central frequency data for the horizontal and vertical planes.

and is added quadratically to the other error. $\alpha = 1.919 \cdot 10^{-3}$ is the momentum compaction factor of the SPS for the tunes used for the measurements.

Systematic effects due to the settings of the horizontal orbit correctors are negligible. The field integral of the orbit correctors was less than 10^{-5} of the total field. Effects due to orbit lengthening [7] are also negligible.

The result for the beam momentum for a nominal settings of 450 GeV/c is given in Table 4. The beam momentum is 449.16 ± 0.14 GeV/c, which is -0.19 ± 0.03% lower than the nominal momentum. This beam momentum corresponds to a measured magnetic field in the SPS reference dipole magnet of 2.0251 ± 0.0002 T. The accuracy on the beam momentum is 0.03% and

Parameter	Value
Proton momentum P (GeV/c)	449.155 ± 0.136
Proton speed β_p	$0.999997818 \pm 0.000000002$
Pb^{53+} ion speed β_{pb}	$0.999966887 \pm 0.000000020$
Central orbit length C (m)	6911.5662 ± 0.0024
Average machine radius $R = C/2\pi$ (m)	1100.0099 ± 0.0004

Table 4: Beam parameters obtained from the central frequency measurements, averaged over the data obtained from the horizontal and vertical planes. The errors are determined from the systematic difference between the data from the two planes. For the beam energy, the contribution due to Equation 13 is included in the error.

it is dominated by the systematic differences between the two planes. The intrinsic accuracy of each measurement is 0.01−0.02%, see Table 3.

The length of the central orbit is 62.4 ± 4.8 mm longer than the nominal length used in the SPS machine model. The corresponding difference for the average machine radius is 9.9 ± 0.4 mm, for a nominal average machine radius of 1100 m. Those results are consistent with previous circumference measurements [8].

5 Discussion

5.1 Machine Circumference

The observed differences in the central frequency for the two planes correspond to a systematic 0.7 mm shift of the radial alignment between the LSF and LSD sextupole families. This number largely exceeds the expected alignment accuracies of 0.2 mm or better. Statistically a systematic alignment difference of much less than 0.1 mm would be expected. The result can be either due to a systematic difference between the sextupole families or to a large shift of a few isolated elements that must therefore have systematic shifts of the order of centimeters. Such large values seem however to be excluded by the vacuum chamber and below tolerances.

The effects of the observed orbit r.m.s. were evaluated with MAD [9]. The predicted central frequency shifts between the two planes can reach 20 Hz, but for the observed orbit pattern, the sign of the predicted shift is opposite to what is observed (higher central frequency in the horizontal plane).

In any case this offset deserves further studies that can be performed on the LHC MD beam at 26 GeV/c.

5.2 Closed Orbit Data Analysis

Closed orbit data were also recorded during the energy calibration experiments to evaluate its possibilities and limitations. From the horizontal closed orbit dependence on the RF frequency it is also possible to determine the frequency for which the beam is centered in the 108 horizontal orbit monitors. This measurement is however delicate due to the sensitivity of the results on the monitor calibration and due to the very small signals (and high noise) for the Pb^{53+} beams. For example all monitors of sextant 3 are not usable with lead beams due to the large RF noise. The proton closed orbit for an almost centered beam is shown in Figure 4 together with the measured difference between proton and Pb^{53+} beams. The orbit difference seems to be mostly due to noise or systematic monitor offsets.

Results from the closed orbit data are in rough agreement with the horizontal tune measurements, but difference of up to ± 40 Hz are observed. The results are very sensitive to the selection of the pickups. For example, including or excluding the monitors that do not work for ions in sextant 3 for the proton orbit data yields differences of 20 Hz for the central frequency.

The main conclusion of the orbit analysis is that the orbit data is not sufficiently reliable to be used as a cross-check of the tune data, but it roughly confirms the central frequency values obtained for the horizontal plane.

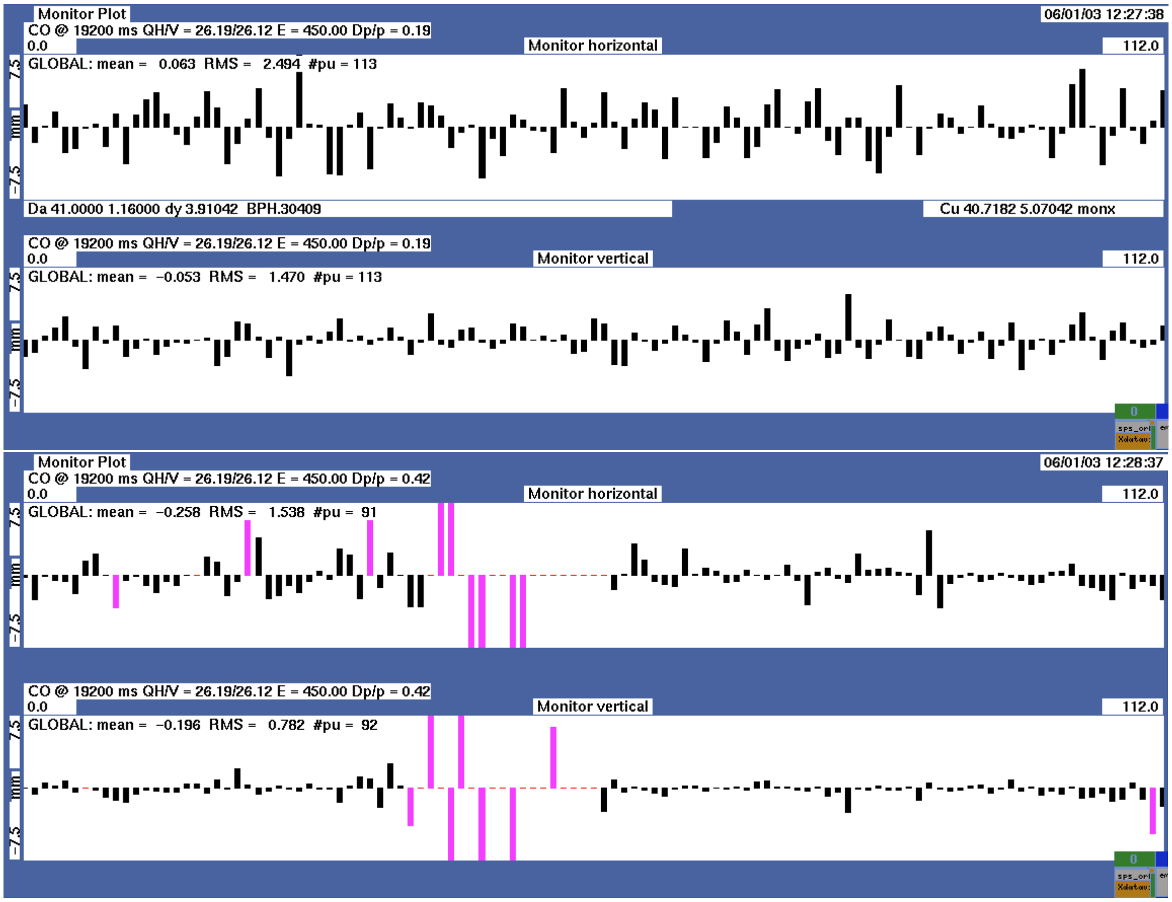

Figure 4: Top : Horizontal and vertical proton beam closed orbit at 450 GeV/c for a radial position close to the central RF frequency. Bottom : closed orbit difference between Pb^{53+} and proton beams at 450 GeV/c for frequency settings where each beam is almost centered in the horizontal monitors. For the Pb^{53+} beam, no monitor in sextant no. 3 gives good signals due to the low intensity and the noise from the RF system. Most of the orbit differences seem to be consistent with noise or monitor offsets.

5.3 Comparison with Earlier Measurements

A similar energy calibration was performed in 1991 to determine the beam momentum for the SPS $p\overline{p}$ collider run at a nominal momentum of 270 GeV/c [8]. The calibration was based on the comparison of the RF frequencies of protons and oxygen ions. Contrary to the present experiment, the central RF frequencies were not determined using the tune dependence on relative momentum offset. The beams were injected and accelerated in the same magnetic cycle, but the RF frequency difference was obtained by centering the beam using the beam orbit monitors and the closed orbit readings. The beam momentum determined in this experiment was 270.550 ± 0.095 GeV/c for a reference magnet field of 1.22632 T. Considering the present experience with the orbit data, the accuracy quoted for the 1991 results seems to be very optimistic. Scaling the momentum result from the present experiment to the field determined in 1991 yields a beam momentum of 271.99 ± 0.14 GeV/c. The two numbers are clearly inconsistent, with a difference close to 10 times the quoted errors. We suppose that the 1992 measurement error could have been under-estimated, in particular since the data collected in the present experiment shows large systematic effects that exclude a precise measurement of the beam energy. Furthermore a large systematic shift was observed with the 1991 data when the beam position monitors were calibrated with proton beams, but this fact was not taken into in account for the error quoted in Reference [8].

6 Conclusion

The SPS central beam momentum was determined for the LHC beam cycle in view of the commissioning of the LHC. The measured beam momentum is 449.16 ± 0.14 GeV/c for a nominal momentum of 450 GeV/c. The magnetic field in the reference magnet was also recorded in order to transport this calibration to other cycles and from one SPS run to the next. Possible effects of the machine and magnet temperature on the beam momentum need to be evaluated, but are difficult to track due to the lack of temperature sensors on the magnets.

An unexpected difference in the machine circumference was observed for measurements with the LSF and LSD sextupole families, indicating systematic difference in the average radial position of the magnetic centers of the sextupoles. The large difference is not understood and will be studied further in the forthcoming SPS run.

To better understand the stability of the reference magnet measurements, it would be very interesting to re-measure the beam energy using the same technique at the end of the SPS run in 2003 using Indium ions.

7 Acknowledgements

We would like to thank D. Manglunki and S. Hancock and their colleagues from the PS RF and OP groups for providing the lead beam at 26 GeV/c. We received precious help from A. Dinius for setting up the NMR measurements of the SPS reference magnets. We thank all colleagues of SL/OP and SL/RF who have contributed to the machine setting up.

References

[1] R. Bailey *et al.*, Proc. of EPAC92, Nice, France.

[2] L. Arnaudon *et al.*, Nucl. Instr. Meth. A 357, 249 (1995).

[3] P. Melchior, *The Tides of the Planet Earth*, 2nd Edition, Pergamon Press (1983).

[4] J. Wenninger, *Observation of radial ring deformations using closed orbits at LEP*, Proc. of PAC99, New York.

[5] K. Hagiwara *et al.*, Phys. Rev. D66, 010001 (2002).
http://pdg.lbl.gov/

[6] G. Audi and A.H. Wapstra, Nucl. Phys A595, 409 (1995).
Atomic Mass Data Center, http://csnwww.in2p3.fr/AMDC/web/nubdisp_en.html.

[7] J. Wenninger, *Orbit Corrector Magnets and Beam Energy*, SL-Note 97-06 OP (1997).

[8] X. Altuna *et al.*, *A Momentum Calibration of the SPS Proton Beam*, CERN SL/92-32 (EA).

[9] H. Grote and F. Iselin, *The MAD Program*, CERN/SL/90-13 Rev. 5, 1996.

[10] C. Hill and M. Chanel, private communications.